Proceedings of the 28th IEEE
EMBS Annual International Conference
New York City, USA, Aug 30-Sept 3, 2006

EIT Images with Improved Spatial Resolution Using a Realistic Head Model

Guoya Dong, Richard Bayford, Hesheng Liu, Ying Zhou, Weili Yan

***Abstract*—A recursive algorithm is presented to improve the spatial resolution of 3-D Electrical Impedance Tomography (EIT) images in a four-shell realistic head model. In this algorithm, the low spatial resolution image derived from the standardized Low resolution electromagnetic tomography algorithm (sLORETA) is chosen to be the initial estimate for the Focal Underdetermined System Solver (FOCUSS), and a shrinking strategy is adopted for adjusting the source space during iteration process in FOCUSS. Images are presented with improved spatial resolution and the algorithm effectiveness is verified on simulated data by setting two perturbations in the movement and visual regions of the brain.**

I. Introduction

ELECTRICAL impedance tomography (EIT) is an imaging method that estimates the internal conductivity distribution of a bounded domain by measuring the surface voltages when current is injected into the domain. The number of boundary measurements at the surface of the bounded region are limited by the signal-to-nose ratio (SNR), and hence the system equations are underdetermined and do not convey enough information to reconstruct the distribution of the conductivity changes uniquely. There are two approaches that can be used to reconstruct the distribution, linear approximations and non-linear, however the non-linear methods require far greater computation. Therefore, only low spatial resolution images can be achieved by conventional linear inverse solvers, such as GVSPM, pseudo-inverse method, sLORETA, etc.

The focal underdetermined system solver (FOCUSS), which is an initialization-dependent recursive algorithm, produces a localized energy solution based on the weighted minimum-norm least-squares (MNLS) solution [1]. Taking the low spatial resolution image as the initial estimate, FOCUSS employs a re-weighting strategy that gradually improves the spatial resolution during the iterations [2].

Manuscript received March 31, 2006. This work was supported by China Postdoctoral Science Foundation (No.2004035618) and Specialized Research Fund for the Doctoral Program of Higher Education, CHINA (No. 20040080008).

Guoya Dong is with Province-Ministry Joint Key Laboratory of Electromagnetic Field and Electrical Apparatus Reliability, Hebei University of Technology, Tianjin, 300130, CHINA. (Phone: 8622-26581524; e-mail: donggya@jsmail.hebut.edu.cn)

Richard Bayford is with Middlesex University, Archway Campus, Furnival Building, Highgate Hill, London N19 3UA, UK

Hesheng Liu is with School of Electrical Engineering and Computer Science, Washington State University, Spokane, WA 99202 USA

Ying Zhou and Weili Yan are with School of Electrical Engineering, Hebei University of Technology, Tianjin, 300130, CHINA..

A combined FOCUSS method that employs a conventional inverse solvers has been shown to improve the spatial resolution of EIT reconstructed images, for simple geometric shapes [3-4]. However the method has not been demonstrated with complex geometries that have large associated system matrices as would be the case if this technique where to be adopted for clinical applications. The combined FOCUSS method uses a low resolution source image derived from sLORETA for the initial estimate of FOCUSS in 3-D EIT [4]. FOCUSS is a local optimizer, therefore a smooth initialization can help the recursive process achieve a solution closer to the global minima. The re-weighting and shrinking strategy of shrinking-FOCUSS gradually improves the spatial resolution based on the initial estimate. This coupled process was termed shrinking sLORETA-FOCUSS.

In this paper, we present a realistic head model containing four shells is used to reconstruct the EIT images with simulated data. The shrinking sLORETA-FOCUSS algorithm is adopted for the improvement of image spatial resolution. The effectiveness of our algorithm in the realistic head model is verified by setting perturbations in the movement and visual regions of the brain, respectively.

II. Methodology

A. EIT Forward Problem

The EIT forward problem is to estimate the potential distribution induced by the current injected at the surface of the target region, where the conductivity σ is already known. Low-frequency (f<50kHz) current injected into the surface gives rise to quasi-static electric fields, which may be computed using electrostatics techniques. To achieve a good approximation, the electric and magnetic fields are decoupled and the local tissue conductivity is assumed real. With these simplifications, electric current in the conductive media is governed by (1)

$$\nabla \cdot (\sigma \nabla \varphi) = 0, \quad \text{in } \Omega \tag{1}$$

where φ is the electric potential and σ is the conductivity of the media.

The boundary conditions are defined as (2),

$$\begin{cases} -\sigma \dfrac{\partial \varphi}{\partial n} = \pm I\delta & \text{at points where current } I \text{ is} \\ & \text{injected through the boudary } \Gamma \\ \sigma \dfrac{\partial \varphi}{\partial n} = 0 & \text{at other points of } \Gamma \end{cases} \tag{2}$$

For the regular geometry, such as the 2-D homogenous and concentric circular model, or the 3-D homogenous and concentric sphere model, there exists an analytic solution for the EIT forward problem [5-6]. For the complex geometry, numerical solutions have to be used for the EIT forward problem, such as Finite Volume Method [7], Finite Element Method and Boundary Element Method.

B. Construction of System Matrix

Based on the normalized sensitivity matrix method [8], EIT is in essence reduced into solving the ill-posed system as in

$$F \cdot C = g \tag{3}$$

where g is the $m\times1$ column vector of the normalized surface voltage measurement, C is the $n\times1$ column vector of the normalized conductivity change in each element, F is the normalized sensitivity matrix which is an $m\times n$ ($m < n$) matrix. In this paper, FVM is used for solving the EIT forward problem to construct the coefficients of F.

C. Shrinking sLORETA-FOCUSS

1) A Standardized LORETA Algorithm (sLORETA): A unique solution to (3) can be achieved by zero-order Tikhonov-Philips regularization, which uses the following cost function:

$$\min_{C}\{\|g - F\cdot C\|^2 + \alpha\|C\|^2\} \tag{4}$$

where α is the regularization parameter.

sLORETA solves the inverse problem by normalizing the minimum norm inverse with the resolution matrix [9]. The explicit solution is given by:

$$\hat{C} = T \cdot g \tag{5}$$

where $\hat{C}$ represents the estimation of conductivity changes and T is

$$T = F^T\left[FF^T + \alpha\, I\right]^{\dagger} \tag{6}$$

For any matrix M, $M^{\dagger}$ denotes its Moore-Penrose pseudo-inverse. Substituting (3) into (5) yields

$$\hat{C} = TFC = F^T\left[FF^T + \alpha\, I\right]^{\dagger} FC = RC \tag{7}$$

where R is the resolution matrix, defined as

$$R = F^T\left[FF^T + \alpha\, I\right]^{\dagger} F \tag{8}$$

The resolution matrix R describes a mapping from the actual conductivity changes to the estimated ones. Ideally, R would be an identity matrix. In reality, it cannot be an identity because of the ill-posed nature of the inverse problem. In this EIT case, the unknown conductivity change is a scalar per element, which may take positive, zero, or negative values. The sLORETA solution is an estimate normalized by the resolution matrix R:

$$C_i = \left(\hat{C}_i\right)^2 \Big/ R_{ii} \tag{9}$$

where the scalar $\hat{C}_i$ is the estimated change of the conductivity at the i^{th} element, R_{ii} is the i^{th} diagonal element of the resolution matrix R in (8), C_i is the i^{th} element estimated by sLORETA.

2) FOCUSS: The original FOCUSS algorithm recursively employs the weighted minimum norm method. Initialized with a low resolution estimate, the FOCUSS algorithm repeats the procedure of weighted minimum norm and recursively adjusts the weighting matrix till most elements of the solution become nearly zero, and thus converges to a localized solution [1]. The weighting matrix W was constructed by taking the previous estimate as its diagonal elements [3]:

$$W_{(k)} = \mathrm{Diag}\left(C_{(k)}\right), k = 0,1,2,...,l \tag{10}$$

where k is the iteration number, $C_{(k)}$ is the vector of normalized conductivity change at the k^{th} iteration, and $W_{(k)}$ is the weighting matrix at the k^{th} iteration which is a $n\times n$ diagonal matrix. The next solution $C_{(k+1)}$ is updated as (11) and (12)

$$q_{(k+1)} = \left(FW_{(k)}\right)^{\dagger} g \tag{11}$$

$$C_{(k+1)} = W_{(k)} q_{(k+1)} \tag{12}$$

Equations (10) and (11) together represent the weighted minimum norm computation and obtain the updated conductivity changes $C_{(k+1)}$ as

$$C_{(k+1)} = W_{(k)}{W_{(k)}}^T F^T (FW_{(k)}{W_{(k)}}^T F^T)^{-1} g \tag{13}$$

2) Shrinking sLORETA-FOCUSS: In 3-D EIT, many more elements are required, which increases the size n of weighting matrix in (13). In each iteration of FOCUSS, the solution is always searched within the entire solution space. The algorithm must repeatedly handle large matrices although the values of many elements in the solution approach zero during the iteration process. The computation time is also increased. The shrinking method has been utilized to address this problem by reducing both the solution space and the weighting matrix in each iteration for a 3-D sphere model [4]. Taking the solution of sLORETA as the initial estimate, the whole procedure is as follows:

a) To estimate the initial distribution of the conductivity changes $C_{(0)}$ in (3) by the sLORETA method.

b) To set k=0, and the threshold t. Shrink the solution space by discarding all weaker elements in $C_{(k)}$ whose values is smaller than the threshold t. Redefine the solution space to be the retained elements by keeping the corresponding elements in $C_{(k)}$ and the corresponding columns in the system matrix F, then

$$C_{(k)} \to C_{s(k)},\ F \to F_{s(k)} \tag{14}$$

Equation (3) is modified by using the shrunk matrices as

$$g_{s(k)} = F_{s(k)} \cdot C_{s(k)} \tag{15}$$

The threshold t is dependent on the needs in practice and can be chosen as a certain percentage of the maximum value in $C_{(k)}$.

c) To construct the weighting matrix W_s and update the solution of conductivity changes to $C_{s(k+1)}$ as

$$W_{s(k)} = \mathrm{Diag}\left(C_{s(k)}\right) \quad (16)$$

$$C_{s(k+1)} = W_{s(k)} W_{s(k)}{}^T F_s^T (F_s W_{s(k)} W_{s(k)}{}^T F_s^T)^{-1} g_s \quad (17)$$

d) Increment k=k+1, and repeat the steps starting from b) until the solution $C_{s(k+1)}$ is approximately static, i.e., $C_{s(k+1)} \approx C_{s(k)}$.

In practice, the solution can be obtained after just a few iterations. However, the reconstructed region could be separated into several small groups or shrunk too much if too many iterations are used.

III. Simulation

In this paper, a 3-D realistic head model grouped into four regions, including scalp, skull, CSF and brain, is adopted to facilitate the simulation. The mesh system consists of 31111 tetrahedral primary elements and 5939 nodes. Conductivities, outer radii and the number of elements for the four layers are listed in Table I [10]. Thirty-one electrodes are arranged on the surface of the scalp in positions based on a modified 10-20 system of EEG electrode placement. By using approximately opposite electrodes for current injection and adjacent electrodes for potential measurement, each image consists of 258 measurements made from different combinations of the 31 electrodes. The injection protocol was developed from which was designed to maximize the sensitivity of impedance changes inside the human head. And adjacent can be in any direction [10]. Fig.1 shows the positions of 31 electrodes from side view, back view and top view, respectively.

To imitate the brain activity in motor and visual cortex, two simulations are carried out. For the first simulation, the two perturbations, including three and four elements, respectively, are located in the motor region of the brain with both radii of about 5mm. Their centers are about 30mm apart paralleled to *y*-axis, as shown in the first column in Fig. 2. For the second simulation, the two perturbations, both including three elements, are located in the visual region of the brain with both radii of about 5mm. Their centers are about 30mm apart paralleled to *x*-axis, as shown in the first column in Fig. 3.

For both Fig. 2 and Fig. 3, the second columns are reconstructed images by the sLORETA alone, and the third columns are images reconstructed by the shrinking sLORETA-FOCUSS. In order to show results clearly, two sections are displayed for each reconstructed image. In Fig. 2, the upper row is the longitudinal section, while the lower row is the transverse section. In Fig. 3, the upper row is the coronal section, while the lower row is the transverse section.

From the reconstructed images we can see that the images reconstructed by the sLORETA alone suffer from low spatial resolution, these two perturbations could not be distinguished in both cases, as shown in the second columns in Fig. 2 and Fig. 3. By adopting the estimate of sLORETA as the initialization for FOCUSS, these two perturbations are distinguished clearly in both cases, as shown in the third columns in Fig. 2 and Fig. 3. The threshold t for shrinking is set to 0.50. The spatial resolution of the reconstructed images has been greatly improved by the shrinking sLORETA-FOCUSS method.

TABLE I
PARAMETER FOR EACH LAYER

Layer	Conductivity (S/m)	Outer Radius (mm)	Number of elements
Scalp	0.44	92	13676
Skull	0.018	87	7364
CSF	1.79	82	3966
Brain	0.25	80	6105

IV. Discussion and Conclusion

In this paper, the shrinking sLORETA–FOCUSS method is used to improve the spatial resolution of 3-D EIT images in a realistic head model. Our algorithm is validated by setting two perturbations in the motor and visual cortex, respectively. EIT images with high spatial resolution have been achieved and the two perturbations are separated distinctively in both cases. In addition, this shrinking strategy is computationally efficient and is able to produce 3-D images in real-time with high spatial resolution. Further studies are underway to investigate the performance in a 3-D real head models with experimental data.

References

[1] Gorodnitsky I F and Rao B D, "Sparse signal reconstruction from limited data using FOCUSS: a re-weighted minimum norm algorithm", *IEEE Trans. Signal Process,* vol.45**,** pp600–16, 1997.

[2] Liu H., Gao X., Schimpf P., Yang F., Gao S., "A recursive algorithm for the 3-dimensional imaging of brain electric activity: Shrinking LORETA-FOCUSS", IEEE trans. Biomed. Eng. vol. 51(10), pp. 1794-1802. 2004.

[3] Dong G, Liu H, Bayford R and et al, "The spatial resolution improvement of EIT images by GVSPM-FOCUSS algorithm", *Physiol. Meas,* vol.25, pp209–25, 2004.

[4] Dong G, Liu H, Bayford R and et al, "Spatial resolution improvement of 3D EIT images by the shrinking sLORETA-FOCUSS algorithm", *Physiol. Meas,* vol.26, no.2, pp. S199-S208, March, 2005.

[5] Dong G, Ge M, Zou J and et al. "Regional Head Conductivity Estimation by the Iterative Sensitivity Matrix Method", *Proceeding of the 2th International IEEE EMBS Conference on Neural Engineering*, Arlington, Virginia, March 16-19, 2005, pp.45-47

[6] T.C.Ferree, K.J.Eriksen and D.M.Tucker, "Regional Head Tissue Conductivity Estimation for Improved EEG Analysis", *IEEE Trans. Biomed. Eng*., vol.47(12), pp.1584-1592, 2000.

[7] Dong G, Zou J, Bayford R, Ma and et al. "The Comparison between FVM and FEM for EIT Forward Problem". *IEEE Trans. on Magn,* vol.41, no.5, pp1468-1471, May, 2005.

[8] Metherall P. Three dimensional electrical impedance tomography of the human thorax, *PhD Thesis* University of Sheffield, 1998.

[9] Pascual-Marqui R. Standardized low resolution brain electromagnetic tomography (sLORETA): technical details, *Methods Find. Exp. Clin. Pharmacol,*pp5-12, 2002. http://www.unizh.ch/keyinst/NewLORETA

[10] Tidswell T, Gibson A, Bayford R and et al, "Three-dimensional electrical impedance tomography of human brain activity", *NeuroImage,* vol.13, pp283–94, 2001

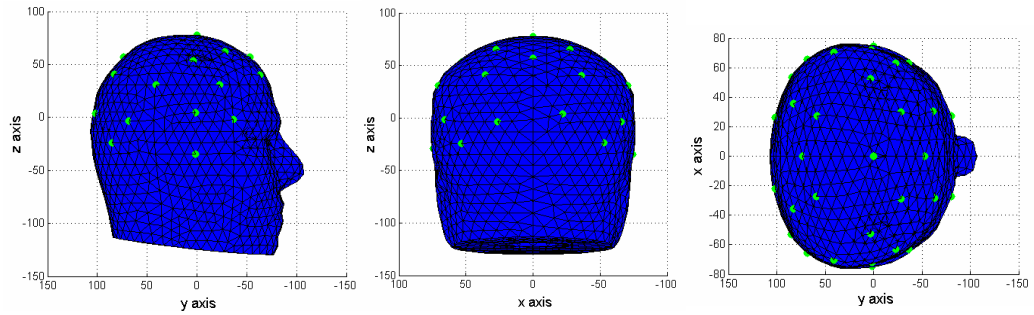

(a) (b) (c)

Fig.1. Illustration of electrode positions (a) Side view (b) Back view (c) Top view

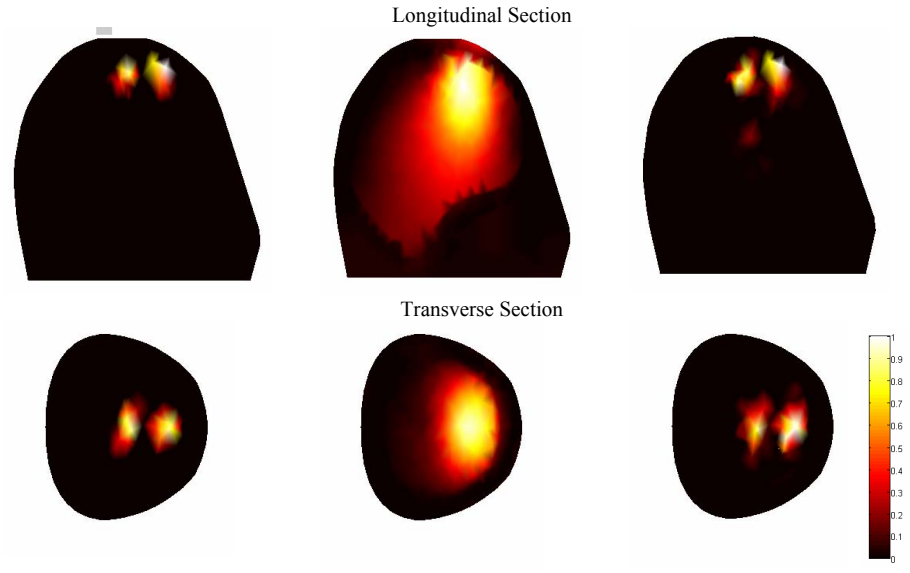

(a) (b) (c)

Fig.2. The reconstructed images with the perturbations located in the movement region of the brain (a) The original distributions of the two perturbations (b) The images reconstructed by the sLORETA alone (c) The images reconstructed by the shrinking sLORETA-FOCUSS.

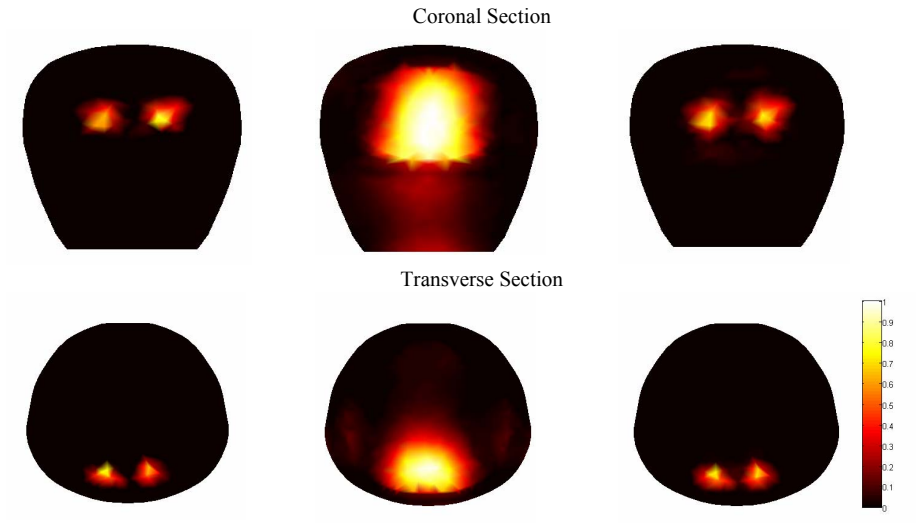

(a) (b) (c)

Fig.3. The reconstructed images with the perturbations located in the visual region of the brain (a) The original distributions of the two perturbations (b) The images reconstructed by the sLORETA alone (c) The images reconstructed by the shrinking sLORETA-FOCUSS.